Journal of Alloys and Compounds 509 (2011) 3419–3424

Contents lists available at ScienceDirect

Journal of Alloys and Compounds

journal homepage: www.elsevier.com/locate/jallcom

Glass fibers templated preparation of TiO_2 microtubes assembled from nano/micro hierarchical TiO_2 crystals

Wei Liu*, Lan Zhang, Li-Xin Cao, Ge Su, Yong-Gang Wang

Institute of Materials Science and Engineering, 238 Songling Road, Ocean University of China, Qingdao, PR China

ARTICLE INFO

Article history:
Received 24 September 2010
Received in revised form
13 December 2010
Accepted 15 December 2010
Available online 23 December 2010

Keywords:
Sol–gel processes
Titanium oxide
Glass fiber
Thin film

ABSTRACT

The unique rutile TiO_2 microtubes with the larger specific surface area and the distinct external/internal surface morphology have been fabricated in large-scale by a sol–gel-hydrothermal method via the readily available glass fibers as templates. The crystal phase, morphology and surface area of as-obtained samples were measured by XRD, SEM, TEM and BET. The results indicate that these microtubes with the inner diameter of ca. 8 μm and the wall thickness of 2–3 μm have a novel double-layer structure, which is built from closely associated TiO_2 rod arrays and TiO_2 gel film. Detailed electric microscopy investigations on such TiO_2 rod arrays exhibit that they are mainly constructed by flower-like rod clusters, and each TiO_2 rod derives from the assembly of the parallel-growth TiO_2 nanowires with the diameter of ca. 10 nm. Such unique hierarchical nano/micro TiO_2 structure enhances the specific surface area of these microtubes effectively, which makes them have more potential applications in the fields of catalysis, sensors, and drug delivery.

1. Introduction

Fabrication of nanoscopic and microscopic hollow tubular structures has attracted significant interests from chemical and material scientists owing to their novel functions in the development of advanced devices and systems [1–8]. Among them, metal oxide microtubes with the hollow interiors exhibit a range of interesting properties including the better monodispersity, chemical stability, operability and less obstruction of hollow interior than their nanosized counterparts, which makes them attractive from both scientific and technological viewpoints in recent years [9–13]. Due to the lesser specific surface area, however, the microtubes usually suffer as compared with the nanotubes in some important special fields, such as catalysis, drug delivery and sensors. Therefore, investigations on improving this disadvantage are very important but challenging. Recently the hierarchical structures based on the assembly of nanoscale building blocks absorb our attention. For instance, hierarchically structured nanowires or nanorods made of TiO_2 [14–28], ZnO [29–32], SnO_2 [33], ZnO/TiO_2 [34], SnO_2/Fe_2O_3 [35], and V_2O_5/TiO_2 [36] have been prepared via various routes. No doubt that abundant voids deriving from the stacking or parallel growth of the building blocks increase the specific surface area to a large extent. However, heretofore few literatures have been concerned on fabricating the tubular hollow structures based on the hierarchical assembly of nanosized building units.

In the strategies to prepare the microtubes, template-assisted technique is the more feasible and effective way [37]. To date, various templates including artificial and natural species have been explored. Yates's group synthesized TiO_2 microtubes by using rod-shaped calcite as template [38]. Additionally, He et al. reported the fabrication of titania microtubes with the porous wall by the replication of human hair [39]. Motojima et al. reported the novel TiO_2 hollow microcoils obtained via the carbon microcoils as the templates [40,41]. Very recent, the microtubes with the core/shell structures have been prepared via electrospun fibers as the soft templates by Jiang's group [42]. Although these tubular structures are successfully obtained, these templates are either infrequent or difficult in preparing. Recent years, the glass fibers, due to their high strengthen, good flexibility, excellent pH stability (excluding HF acid) and very low cost, are considered as one particularly desirable template for the applications in the large-scale synthesis of new functional tubular materials. For example, the various polymer microtubes were prepared based on the glass fibers by Anderson and co-workers [43] and Fery and co-workers [44]. Yang et al. reported the successful fabrication of large-scale uniform silver and copper nano/microtubes by using glass fibers as templates [45]. Herein, we report a facile approach to fabricate large-scale TiO_2 microtubes with the high length-diameter ratio by using low-cost glass fibers as templates. Different to TiO_2 microtubes mentioned above, this tubular structure derives mainly from the hierarchical nano/micro TiO_2 structures on the surface of glass fibers. Such kind

* Corresponding author. Tel.: +86 532 66781690; fax: +86 532 66781334.
E-mail address: weiliu@ouc.edu.cn (W. Liu).

0925-8388/$ – see front matter © 2010 Elsevier B.V. All rights reserved.
doi:10.1016/j.jallcom.2010.12.113

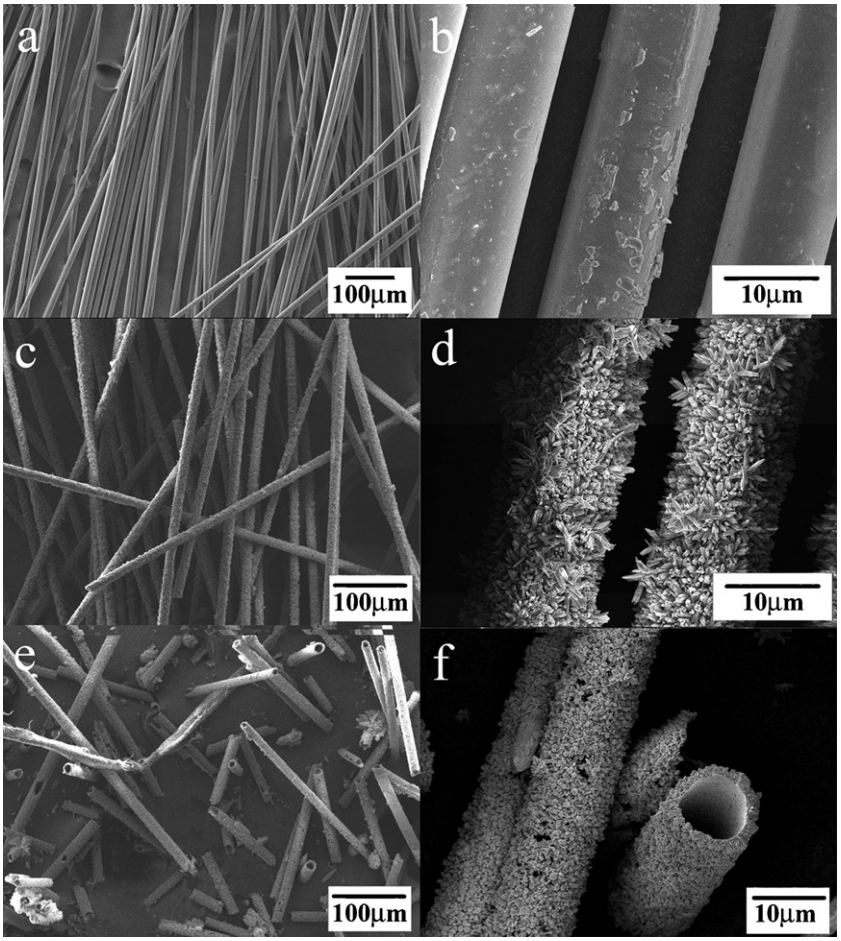

Fig. 1. Low- and high-magnification SEM images of (a and b) the glass fibers with TiO_2 gel film; (c and d) the glass fibers with TiO_2 gel film after hydrothermal treatment and (e and f) the TiO_2 microtubes.

of the stacking or parallel growth of the building blocks increases further the specific surface area of these microtubes, and hence accelerates their potential applications in the fields of catalysis, sensors, and drug delivery.

2. Experimental

Titanium n-butoxide [$Ti(OC_4H_9)_4$], ethanol, hydrochloric acid, polyethylene glycol, hydrofluoric acid (HF, 48%) and acetone were purchased from Sinopharm Chemical Reagent Company in the highest available purity and used without further purification. Commercial amorphous glass fibers with the average diameter of 10 μm (Taishan Fiberglass Inc.) were ultrasonic cleaned by ethanol and nitric acid to get rid of the impurity, and then dried in the oven at 70 °C after rinsed with distilled water for three times. The micro/nano structures on the surface of the glass fibers were fabricated via the sol–gel technology and hydrothermal method. A typical experimental procedure was described as follows. Firstly, a semitransparent TiO_2 sol was formed through continuously stirring a mixed solution, composed of ethanol, tetrabutyltitanate, water and polyethylene glycol in the molar ratio of 12:3:1:3 for 1 h. Secondly, after being soaked in the resultant sol for 1 min under ultrasonic, the well-cleaned glass fibers were pulled up and placed vertically in the oven at 100 °C for half hour. Such sol–gel cycles were repeated for four times. Thirdly, the suitably-sized glass fibers coated with TiO_2 gel were put into an autoclave containing a $Ti(OBu)_4$–HCl–H_2O solution and hydrothermally treated at 150 °C for various time to obtain the hierarchical TiO_2 rod arrays on the glass fibers. Finally, the well-defined TiO_2 microtubes were freed from the templates by dissolving in 24 wt.% HF for 24 h to fully get rid of the glass fibers.

The powder X-ray diffraction (XRD) patterns of as-synthesized samples were measured on a X-ray diffractometer (Bruker D8 ADVANCE) using monochromatized Cu Kα (λ = 0.15418 nm) radiation under 40 kV and 100 mA. The morphologies and microstructures of as-prepared samples were examined with a scanning electron microscopy (SEM, JSM-6700F) and equipped with an energy-dispersive X-ray spectroscope (EDS). Transmission electron microscopy (TEM) observations were carried out on a JEOL JEM-2100 instrument with accelerating voltage of 200 kV in bright-field and selected-area electron diffraction (SAED) modes. The specimens used for TEM studies were dispersed in absolute ethanol by ultrasonic treatment. Nitrogen adsorption–desorption measurements were conducted on a Micromeritics Tristar 3000 analyzer after the samples were degassed at 200 °C for 6 h. The Brunauer–Emmett–Teller (BET) surface area was estimated using adsorption data.

3. Results and discussion

Fig. 1a gives the typical SEM image of the glass fibers coated with TiO_2 gel film. It shows that the glass fibers used here are generally very long and the diameter is in the range of ca. 10 μm. Magnified image (Fig. 1b) exhibits that TiO_2 gel film on the surface of glass fibers are smooth and no obvious splits can be observed except for some small uplifts, displaying the good adhesion between the glass fibers and the TiO_2 gel film. After hydrothermal treatment, these glass fibers become opaque white but still keep good mechanic strengthen (Fig. S1). Accompanying with the distinct surface morphology and microstructure modification of the glass fibers, the diameter enlargement of such fibers can also be noticed (Fig. 1c). A close observation shows that a mass of TiO_2 rods with the length of ca. 1 μm grow densely on the surface of the glass fibers, forming a large area of crystal rod array to cover the whole surface of glass fibers (Fig. 1d). After the glass fiber templates are removed by HF acid, the microtubes with the hollow interior can be obtained, though parts of these tubular fibers have been broken due to their brittleness (Fig. 1e). The cross-sectional view of such microtubes (Fig. 1f) exhibits that the glass fibers can be completely removed by the corrosion of HF acid, giving rise to the formation of the microscopic tubular structure with the inner diameter of ca. 8 μm and the wall thickness of ca. 2.5 μm.

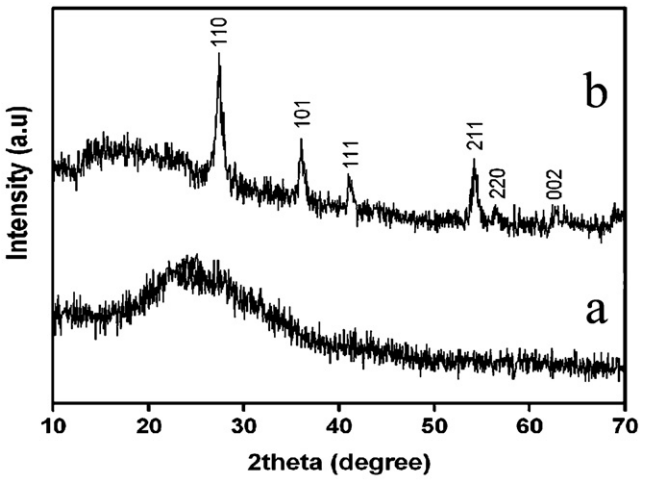

Fig. 2. XRD patterns of (a) the glass fibers with TiO_2 gel film and (b) the TiO_2 microtubes.

The phase and purity of the glass fibers coated with the TiO_2 gel film and the TiO_2 microtubes were investigated by the XRD measurement. The XRD pattern of the glass fibers with the TiO_2 gel film (Fig. 2a) shows a sole broad peak in the 2θ angle range from 15° to 35°, which is ascribed to the amorphous phase of the glass substrate. No other peaks in the pattern reveal that TiO_2 gel film on the glass fibers is amorphous. The XRD pattern of TiO_2 microtubes (Fig. 2b) displays that all the peaks can be readily indexed as pure tetragonal rutile phase (PDF no. 65-0190), indicating that the TiO_2 nanorod arrays formed on the surface of glass fibers in the hydrothermal process are rutile crystalline phase.

Fig. 3 shows the typical SEM images of the rutile TiO_2 microtubes grown at 150 °C for 4 h. Differing to other microtubes reported previously, as-made TiO_2 microtubes exhibit a hollow tubular structure with the distinct internal/external surface morphologies. As shown in the magnified SEM photo (Fig. 3a), the entire outer surface of such microtubes has been covered uniformly by the TiO_2 rod arrays to form the rough external surface, whereas the internal surface is relatively smooth. The further enlarged view (Fig. 3b) of the microtubes demonstrates the double-layer structure of the microtube wall, which can be constituted of the TiO_2 rod array layer and the gel film layer. Since the TiO_2 gel film layer is very thin, the tubular structure can also be described as the self-rolling formation of TiO_2 rod arrays. Actually, this novel external/internal surface morphological diversity is mainly attributed to the two various preparing stages of such microtubes. The smooth internal surface reviews the feature of TiO_2 gel film produced by sol–gel method, while the rough external surface constructed by the TiO_2 rod arrays is formed in the subsequent hydrothermal process.

Although having the low proportion in the microtubes, TiO_2 gel film layer has the strong impact on the formation of these TiO_2 microtubes. The corresponding experimental results have proved that TiO_2 rod crystals cannot grow successfully on the surface of the glass fibers without the existence of TiO_2 gel film. This can be explained that the smooth surface of the amorphous glass fibers cannot apply for stable nucleation sites for TiO_2 nuclei. Few tiny holes on the microtube surface can be further confirmed it (Fig. 3c),

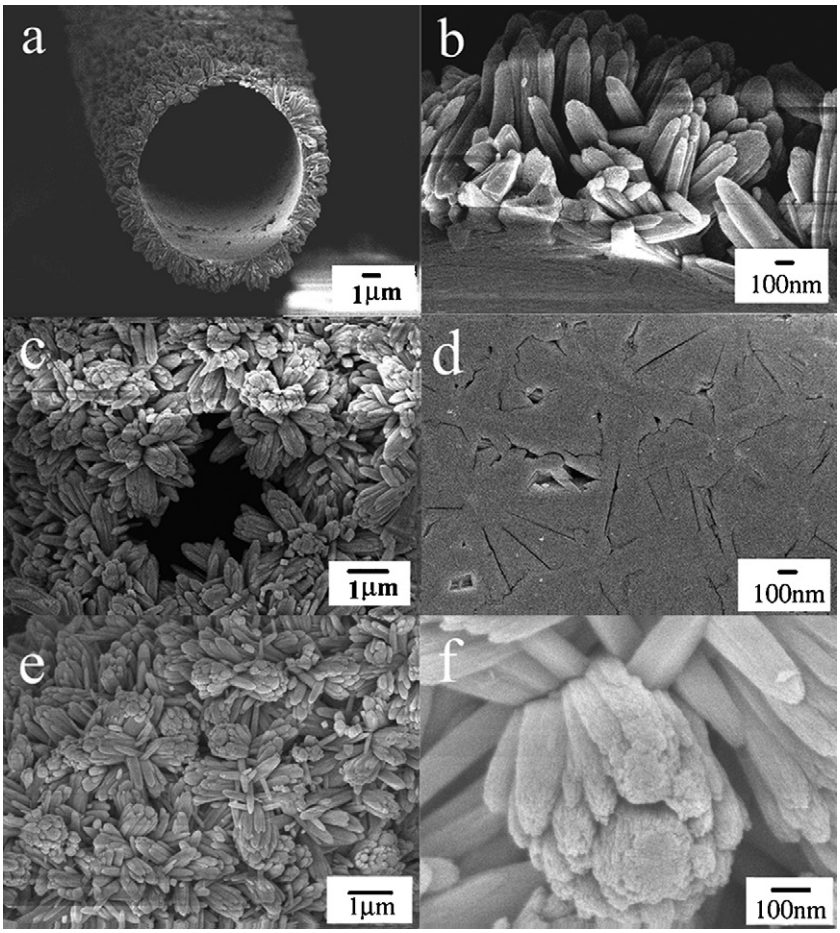

Fig. 3. (a) Cross-sectional SEM image of the TiO_2 microtubes; (b) close observation of the wall of as-made microtubes; (c) SEM image of the hole on the surface of the microtubes; (d and e) high magnification SEM photos of the outer surface and inner surface; (f) SEM image of the flower-like rod clusters.

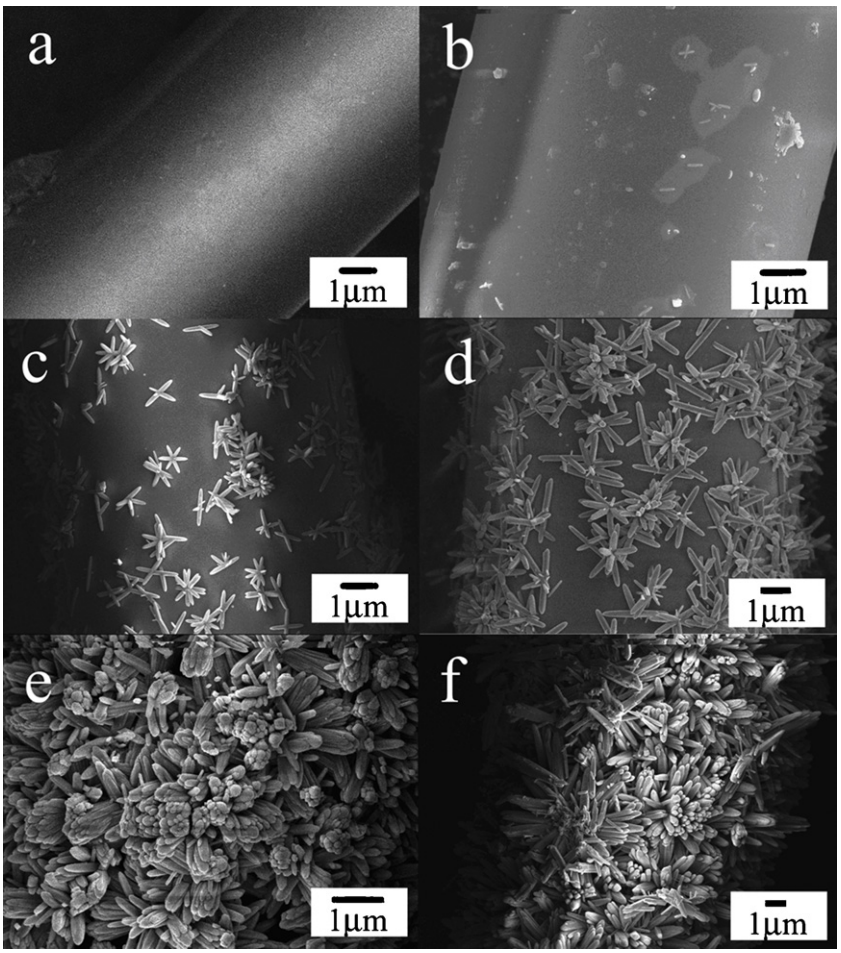

Fig. 4. SEM image of the glass fibers with the TiO_2 gel film (a) and the time-dependence SEM images of growing hierarchical TiO_2 structures after hydrothermal treatment for (b) 1 h, (c) 2 h,(d) 3 h, (e) 4 h and (f) 8 h.

because they may derive from the coating inhomogeneity of TiO_2 gel. Although TiO_2 gel are amorphous, the organic groups of TiO_2 gel can form the chemical bonding with the amounts of $Ti(OBu)_4$, and hence accelerate the heterogeneous nucleation and the growth of TiO_2 crystals on the surface. The inner surface morphology of these microtubes (Fig. 3d) shows that there are amounts of streaks distributed randomly in the TiO_2 gel film layer, possibly resulting from the stress effect of the growing TiO_2 rod crystals under hydrothermal conditions. The close observation of the external surface (Fig. 3e) reveals that TiO_2 rods grow radially on the TiO_2 gel film in the random pattern. The TiO_2 rods are tetragonal in shape with the apical top. One interesting point is the discovery of a novel flower-like growth pattern of TiO_2 rods. This kind of flower-like rod clusters is constructed by the various kinds of crystal rods, which can be classified with petal-like, stamen-like and pistil-like ones, illustrated by Fig. 3f. As the pistil-like rods, a large cylindrical crystal occupies the center of the flower-like rod cluster. Around it, several stamen rods with the small size grow in parallel and closely surround the pistil-like rods, forming together the heart of the flower-like cluster. Being nearly perpendicular to the stamen and pistil rods, the petal rods grow out from the center of the clusters and extend along the surface of the substrate, giving rise to the formation of the whole flower-like structure. Abundant of such flower-like clusters distribute compactly on the surface and form the external nanorod layers, which further construct the hollow tubular structure with TiO_2 gel layers.

Although as-obtained TiO_2 microtubes exhibit the complex hierarchical structures, the surfacial microstructue and morphology of these microtubes can be easily controlled by changing the experimental parameters, such as reaction time. The growth process of TiO_2 rods on the surface of TiO_2 gel films is demonstrated in Fig. 4, showing the dependence of the rutile TiO_2 rod scales with the reaction time. Fig. 4a displays that the homogenous coating of TiO_2 sol on the surface of glass fibers leads to a smooth TiO_2 gel layer. After hydrothermal treated for 1 h, a few of tiny protuberances appear distinctly on the surface of the TiO_2 gel film and serve as the original crystal seeds to further guide the TiO_2 rods' subsequent growth (Fig. 4b). Part of them have further evolved into small nanorods with the length of ca. 500 nm and the diameter of ca. 100 nm as seen in Fig. S2. When the time increases to 2 h, amounts of TiO_2 rods with the flower-like structure appear and occupy the large area of the TiO_2 gel film surface (Fig. 4c). Besides the flower-like structure, we also observe the cross-like and three-leg structures with the relatively low proportion. After hydrothermally treating for 3 h, the petal of such rod flowers grow longer enough to intersect with those of the neighboring flowers, resulting in a net-like structure of nanorods (Fig. 4d). At the same time, more branched rod crystals start to grow from the central long rod (Fig. S3), giving rise to the more compact flower-like structure. Due to the growth of individual and branched rods, the TiO_2 gel film has been covered completely by the unaligned TiO_2 rod array as seen in Fig. 4e. Prolonging the duration to 8 h, the length and the diameter of the TiO_2 rods further increase to ca. 5 μm and 1 μm, respectively (Fig. 4f). Generally, both the length and diameter of the TiO_2 rods augment proportionately with the increase of the hydrothermal reaction time, which means that it is feasi-

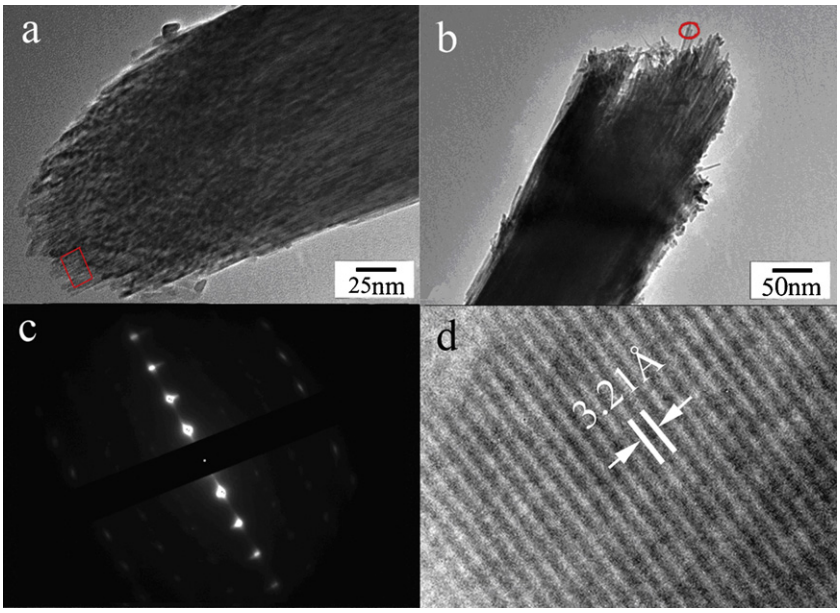

Fig. 5. TEM images of (a) the top part and (b) the end part of a single TiO_2 rod; (c) SAED pattern obtained from the top (rectangle) of the TiO_2 rod; (d) High-resolution TEM image recorded from a single nanowire of the end part of the TiO_2 rod (circle).

ble to control product morphologies by simply tuning the reaction time.

Transmission electron microscopy (TEM) and electron diffraction (ED) analysis were examined to further investigate the growth habits of these TiO_2 rods. As shown in Fig. 5a, a typical TEM image taken from an individual rod shows that the TiO_2 rods are not single crystalline, but the assembly of a large amount of TiO_2 nanowires with oriented attachment. As seen in the SEM view of the end part of the TiO_2 rod (Fig. 5b), some detached nanowires appear at the fracture part of the rods. These nanowires are very thin and the average diameter is ca. 10 nm. The selected area ED patterns from one rod (SAED, Fig. 5c) show that such rod has the single crystal feature due to only a few isolated symmetrical spots in the diffraction patterns, which indicates that the nanowires are packed in a highly ordered manner. High-resolution TEM image of one single TiO_2 nanowire is shown in Fig. 5d. The lattice fringes indicate that TiO_2 nanowires are well crystallized. The spacing between two fringes is 0.321 nm, corresponding to the interplanar distance of the (1 1 0) index planes of the rutile TiO_2, indicating that as-prepared TiO_2 rods via hydrothermal approach are the rutile structure, which is consistent with the result of XRD. Furthermore, it is observed that the (1 1 0) crystal planes are perpendicular to the *c*-axis, which suggests that TiO_2 nanowires grow along the [0 0 1] direction. As is well known, the rutile TiO_2 crystal structure is built of TiO_6 octahedra chains along the *c*-axis [46]. According to PBC theory [47,48], the direction of the strongest chemical bond is usually the direction in which the crystal has the fastest growth velocity. Due to the stronger chemical bonds in the TiO_6 octahedral chains than those between the chains, for rutile TiO_2 crystal, the growth velocity along the [0 0 1] direction is faster than that of the [1 1 0] direction, giving rise to the formation of the rutile TiO_2 crystal rod arrays.

This kind of double-layer microtubular structure endows as-obtained TiO_2 microtubes with more unique feature. In term of the specific surface area, the rather rough external surface built of the crystal rod arrays extends effectively the specific surface area of these microtubes. The BET analysis indicates that the specific surface area of as-obtained TiO_2 microtubes can reach to 60 m^2/g, corresponding to 1.42 m^2/g for the glass fibers with the TiO_2 gel. Therefore, the enlargement of the surface area will enhance conspicuously the potentials of such microtubes in the large-scale applications as catalyst carriers, sensors, and sorbents. On the other hand, the distinct external/internal surface microstructures of these microtubes achieve possibly the simultaneous delivery for various drugs. Especially for their distinctive mesocrystalline structure of the external surface, small molecules may be able to penetrate the TiO_2 rods through the mesoscale interstices among the nanowires.

4. Conclusions

The novel TiO_2 microtubes with the inner diameter of ca. 8 μm and the wall thickness of 2–3 μm have been successfully prepared in large-scale via the glass fiber templates by using of the sol–gel and hydrothermal methods. Differing to other tubular structures, the microtubes reported here have the unique double-layer structure, the thick outer layer of which is constructed by the thick rutile TiO_2 nanorod arrays, and the thin inner layer of which is made by TiO_2 gel film. Such close attached double layers endow these microtubes the unique surface morphology. In the TiO_2 crystal rod array, the novel flower-like TiO_2 rod clusters, made of petal-like, stamen-like and pistil-like rods, are observed for the first time. Additionally, it is also found that these TiO_2 crystal rods are not single crystalline, but the assembly of abundant of the parallel growing TiO_2 nanowires with the average diameter of ca. 10 nm. Such hierarchical nano/micro TiO_2 structures enhances the specific surface area of as-made TiO_2 microtubes effectively, which makes them have much bigger potentials in the large-scale applications as catalyst carriers, sensors, sorbents and drug delivery. Besides TiO_2, the similar hierarchical nano/micro tubular structures of other meal oxides such as ZnO, SnO_2, CuO, even heterogeneous ones, can also be facile fabricated via the same method.

Acknowledgements

This work was supported by the Program for New Century Excellent Talents in University (NCET-08-0511) and the Promotive research fund for excellent young and middle-aged scientists of Shandong Province (BS2010CL049).

Appendix A. Supplementary data

Supplementary data associated with this article can be found, in the online version, at doi:10.1016/j.jallcom.2010.12.113.

References

[1] Y. Xia, P. Yang, Y. Sun, Y. Wu, B. Mayers, B. Gates, Y. Yin, F. Kim, H. Yan, Adv. Mater. 15 (2003) 353–389.
[2] S.Z. Chu, S. Inoue, K. Wada, D. Li, H. Haneda, S. Awatsu, J. Phys. Chem. B 107 (2003) 6586–6589.
[3] M. Wang, D.J. Guo, H.L. Li, J. Solid State Chem. 178 (2005) 1996–2000.
[4] L. Qian, Z.S. Jin, S.Y. Yang, Z.L. Du, X.R. Xu, Chem. Mater. 17 (2005) 5334–5338.
[5] F.Z. Song, X.Q. Shen, J. Xiang, Y.W. Zhu, J. Alloys Compd. 507 (2010) 297–301.
[6] O.K. Varghese, D. Gong, M. Paulose, K.G. Ong, E.C. Dickey, C.A. Grimes, Adv. Mater. 15 (2003) 624–627.
[7] M. Paulose, O.K. Varghese, G.K. Mor, C.A. Grimes, K.G. Ong, Nanotechnology 17 (2006) 398–402.
[8] H.J. Zhang, F. Ye, L.M. Liu, H.F. Xu, C. Sun, J. Alloys Compd. 504 (2010) 171–1761.
[9] B. Liu, S. Wei, Y. Xing, D. Liu, Z. Shi, X. Liu, X. Sun, S. Hou, Z. Su, Chem. Eur. J. 16 (2010) 6625–6631.
[10] X. Guo, J. Yang, Y. Deng, H. Wei, D. Zhao, Eur. J. Inorg. Chem. (2010) 1736–1742.
[11] K. Dietrich, C. Strelow, C. Schliehe, C. Heyn, A. Stemmann, S. Schwaiger, S. Mendach, A. Mews, H. Weller, D. Heitmann, T. Kipp, Nano Lett. 10 (2010) 627–631.
[12] K. Kumar, B. Nandan, V. Luchnikov, E. Gowd, M. Stamm, Langmuir 25 (2009) 7667–7674.
[13] X.Z. Zhang, B. Lin, Y.H. Ling, Y.C. Dong, D. Fang, G.Y. Meng, X.Q. Liu, J. Alloys Compd. 494 (2010) 366–371.
[14] C. Sun, N. Wang, S. Zhou, X. Hu, S. Zhou, P. Chen, Chem. Commun. (2008) 3293–3294.
[15] L. Wang, T.T. Zhao, Z. Zhang, G. Li, J. Nanosci. Nanotechnol. 10 (2010) 8312–8321.
[16] B.E. Heredia-Cervera, S.A. González-Azcorra, G. Rodríguez-Gattorno, T. López, E. Ortiz-Islas, G. Oskam, Sci. Adv. Mater. 1 (2009) 63–68.
[17] S. Li, Q.H. Shen, J.J. Zong, H. Yang, J. Alloys Compd. 508 (2010) 99–105.
[18] M.Z. Tang, J.M. Wu, Sci. Adv. Mater. 1 (2009) 144–152.
[19] D.P. Singh, N. Ali, Sci. Adv. Mater. 2 (2010) 295–335.
[20] Y. Zhou, Sci. Adv. Mater. 2 (2010) 359–364.
[21] Y.H. Ling, J.S. Liao, X.Y. Liu, X.M. Wu, X.D. Bai, J. Nanosci. Nanotechnol. 10 (2010) 7020–7024.
[22] T. Kawai, H. Takahashi, Y. Matsushima, T. Ogata, H. Unuma, Sci. Adv. Mater. 2 (2010) 74–78.
[23] M. Inada, K. Mizue, N. Enomoto, J. Hojo, Sci. Adv. Mater. 2 (2010) 102–106.
[24] X. Cao, X. Xue, Sci. Adv. Mater. 2 (2010) 390–395.
[25] D. Chu, Y. Zeng, D. Jiang, Y. Masuda, Sci. Adv. Mater. 1 (2009) 227–229.
[26] Y. Masuda, Y. Jinbo, K. Koumoto, Sci. Adv. Mater. 1 (2009) 138–143.
[27] Y. Wu, J. Yu, H.M. Liu, B.Q. Xu, J. Nanosci. Nanotechnol. 10 (2010) 6707–6719.
[28] R. Scotti, I.R. Bellobono, C. Canevali, C. Cannas, M. Catti, M.D. Arienzo, A. Musinu, S. Polizzi, M. Sommariva, A. Testino, F. Morazzoni, Chem. Mater. 20 (2008) 4051–4061.
[29] L. Xu, Y. Guo, Q. Liao, J. Zhang, D. Xu, P. Chen, J. Phys. Chem. B 109 (2005) 13519–13522.
[30] G. Li, X. Lu, D. Qu, C. Yao, F. Zheng, Q. Bu, C. Dawa, Y. Tong, J. Phys. Chem. C 111 (2007) 6678–6683.
[31] L. Xu, Q. Chen, D. Xu, J. Phys. Chem. C 111 (2007) 11560–11565.
[32] T. Sounart, J. Liu, A. Voigt, M. Huo, E. Spoerke, B. Kenzie, J. Am. Chem. Soc. 129 (2007) 15786–15793.
[33] H. Ohgi, T. Maeda, E. Hosono, S. Fujihara, H. Imai, Cryst. Growth Des. 5 (2005) 1079–1083.
[34] N. Wang, C. Sun, Y. Zhao, S. Zhou, P. Chen, L. Jiang, J. Mater. Chem. 18 (2008) 3909–3911.
[35] D. Zhang, L. Sun, C. Jia, Z. Yan, L. You, C. Yan, J. Am. Chem. Soc. 127 (2005) 13492–13493.
[36] R. Ostermann, D. Li, Y. Yin, T. McCann, Y. Xia, Nano Lett. 6 (2006) 1297–1302.
[37] G. Kim, S. Lee, G. Michler, H. Roggendorf, U. Gosele, M. Knez, Chem. Mater. 20 (2008) 3085–3091.
[38] D. Liu, M. Yates, Langmuir 23 (2007) 10333–10341.
[39] S. Liu, J. He, J. Am. Ceram. Soc. 88 (2005) 3513–3514.
[40] S. Motojima, T. Suzuki, Y. Noda, A. Hiraga, H. Iwanaga, T. Hashishin, Y. Hishikawa, S. Yang, X. Chen, Chem. Phys. Lett. 378 (2003) 111–116.
[41] S. Motjima, T. Suzuki, Y. Noda, A. Hiraga, S. Yang, X. Chen, T. Hashishin, Y. Hishikawa, J. Mater. Sci. 39 (2004) 2663–2674.
[42] H. Chen, N. Wang, J. Di, Y. Zhao, Y. Song, L. Jiang, Langmuir 26 (2010) 11291–11296.
[43] D. Tuncel, J. Matthews, H. Anderson, Adv. Funct. Mater. 14 (2004) 851–855.
[44] R. Mueller, L. Daehne, A. Fery, Polymer 48 (2007) 2520–2525.
[45] X. Yang, X. Zhu, L. Yuan, J. Sun, Y. Liang, J. Mater. Sci. 44 (2009) 3382–3386.
[46] X. Bokhimi, A. Morales, M. Aguilar, J.A. Toledo-Antonio, F. Pedraza, Int. J. Hydrogen Energy 26 (2001) 1279–1287.
[47] P. Hartman, W.G. Perdok, Acta Crystallogr. 8 (1955) 49–52.
[48] P. Hartman, W.G. Perdok, Acta Crystallogr. 8 (1955) 521–524.